Biotechnology Reports 10 (2016) 49–55

Contents lists available at ScienceDirect

Biotechnology Reports

journal homepage: www.elsevier.com/locate/btre

Immobilization of ω-transaminase by magnetic PVA-Fe_3O_4 nanoparticles

Honghua Jia*, Fan Huang, Zhen Gao, Chao Zhong, Hua Zhou, Min Jiang, Ping Wei

College of Biotechnology and Pharmaceutical Engineering, Nanjing Tech University, Nanjing 211800, China

ARTICLE INFO

Article history:
Received 12 February 2016
Received in revised form 8 March 2016
Accepted 9 March 2016
Available online 11 March 2016

Keywords:
ω-transaminase
Magnetic PVA-Fe_3O_4 nanoparticles
Immobilization
Chiral amine

ABSTRACT

ω-Transaminase (ω-TA) as a kind of important biocatalyst is widely used in preparation of chiral intermediates. In this paper, a magnetic PVA-Fe_3O_4 nanoparticles was prepared and employed on immobilization of ω-TA to reduce the cost, increase reusability and enhance stability. The prepared magnetic PVA-Fe_3O_4 nanoparticles were characterized by transmission electron microscope (TEM), X-ray diffraction (XRD) and vibrating sample magnetometer (VSM). The average size of magnetic PVA-Fe_3O_4 nanoparticles was located between 30–40 nm ω-TA was immobilized onto magnetic PVA-Fe_3O_4 nanoparticles via glutaraldehyde cross-linking, achieving a wider pH range as 6–8 and also a better thermal stability at 60 °C. Meanwhile, the immobilized ω-TA could be successfully reused for 13 times in biotransformation. These results therefore indicated that the immobilized ω-TA with high stability might be readily utilized in industrial purposes.

1. Introduction

ω-Transaminase (ω-TA), which is a pyridoxal-5′-phosphate (PLP) dependent enzyme, plays a very important role in synthesis of chiral amines and non-natural amino acids [1–3]. Processes catalyzed by ω-TA are advantageous over others with high enantioselectivity, precise regioselectivity, and broad substrate specificity [4]. Previously, application of ω-TA was sometimes restricted by its stability, production cost and difficulty in recycling. In order to overcome such problem, many efforts have been made, such as over-expression of ω-TA in *E. coli* to reduce the production cost and the addition of DMSO as cosolvent to improve the stability of ω-TA at 50 °C for industrial application [5,6]. For now, more attention is given to the immobilization of enzymes, which might improve the stability and also allow for recycling of the enzymes.

Over the past years, scientists have managed to immobilize ω-TAs onto different supports. ω-TA had been entrapped into calcium alginate, showing increase in V_{max} by 28–33% and decrease in activation energy by 41% compared to the free [7]. By means of binding with chitosan covalently, immobilized ω-TAs had retained higher activity and significant stability compared with the free enzyme [8,9]. Sol–gel/Celite 545 was also tested as a matrix to immobilize commercially available ω-TA, and the immobilized ω-TA maintained its activity at a broader pH range and better operational stability without any substantial loss in enantioselectivity and conversion in five cycles [10]. Immobilized ω-TA on SEPABEADS EXE120 demonstrated its good capability of operating in organic solvent and also excellent recyclability [11]. Besides, whole cells containing ω-TA were also immobilized onto different carriers, indicating improved storage and operational stability [12,13].

In consideration of high load rate, specific surface area, and intensity, nanomaterials have been considered as the promising carriers for enzyme immobilization [14]. Moreover, much research has revealed that nanomaterials can provide better microenvironments surrounding enzyme molecules and bring about much improved performances (e.g. stabilities) [15]. Investigations on immobilized enzymes supported by nanomaterials with types of spheres, fibers, and tubes have been dramatically increased [16–18]. Among them, functionalized magnetic nanomaterials are found to be a practically useful support for enzyme immobilization due to readily recyclability [19]. Some papers have been reported to be involved in enzymes immobilized onto magnetic nanomaterials. Laccase, cholesterol oxidase, alcohol dehydrogenase, lipase, etc, have been immobilized onto different magnetic nanomaterials and exhibited good stability and reusability [20–23]. However, seldom have studies been carried out related with immobilization of ω-TA onto magnetic nanoparticles.

In the present study, Fe_3O_4-PVA was prepared and applied in immobilization of ω-TA. XRD and TEM were employed to analyze Fe_3O_4 and Fe_3O_4-PVA nanoparticles. The immobilized ω-TA was

* Corresponding author.
E-mail address: hhjia@njtech.edu.cn (H. Jia).

http://dx.doi.org/10.1016/j.btre.2016.03.004

characterized by enzymatic parameters. Still the reusability of immobilized ω-TA was investigated.

2. Materials and methods

2.1. Materials

The recombinant ω-TA (E.C. 2.6.1.1) originated from *Mycobacterium vanbaalenii* was purchased from Sigma–Aldrich. Polyvinyl alcohol (PVA, 1750 ± 50), ferric chloride hexahydrate ($FeCl_3 \cdot 6H_2O$), ferrous chloride tetrahydrate ($FeCl_2 \cdot 4H_2O$), concentrated hydrochloric acid, 25% glutaraldehyde, *n*-butanol, benzoyl peroxide, dodecyl trimethyl ammonium chloride, Tween 80, Coomassie Brilliant Blue G250 and bovine serum albumin were obtained from Sinopharm. Pyridoxal-5′-phosphate (PLP), *R*-α-methylbenzylamine (*R*-α-MBA) were supplied by Aladdin. Edible oil was purchased from a local firm. All other reagents used were of analytic grade.

2.2. Preparation of magnetic Fe_3O_4 nanoparticles

Three and half milliliter of concentrated hydrochloric acid, 7.96 g of $FeCl_2 \cdot 4H_2O$ and 10.82 g of $FeCl_3 \cdot 6H_2O$ were dissolved and mixed in 100 mL of distilled water. After 30 min of nitrogen purging, the solution was heated at 70 °C and 500 mL of 3 M NaOH was slowly dropped with mechanical agitation at 500 rpm under a nitrogen atmosphere. After 1 h of reaction, the product was isolated with an external magnetic field and rinsed with distilled water until neutral. Finally, the product was rinsed three to five times with methanol and suspended in methanol at a concentration of 0.01 g/mL.

2.3. Preparation of magnetic PVA-Fe_3O_4 nanoparticles

Under nitrogen atmosphere, 500 mL of 0.01 g/mL Fe_3O_4 nanoparticles fluid was added into a flask at 70 °C, and 1.5 g of dodecyltrimethylammonium methyl chloride and 15 mL of *n*-butanol was then dropped into mixture. With continually mechanical stirring, 60 mL of PVA solution (10%, w/v) was added into the solution. Thirty minutes later, 2 g of initiator of benzoyl peroxide dissolved in 10 mL of ethanol was added under mechanical stirring at 70 °C. After 7 h of reaction, the product was separated employing a magnetic field and rinsed 3 times with distilled water, followed by being rinsed with methanol and dried in an oven at 75–80 °C for 4 h.

2.4. Characterization of magnetic Fe_3O_4 and PVA- Fe_3O_4 nanoparticles

The size and morphology of magnetic Fe_3O_4 and PVA-Fe_3O_4 nanoparticles were characterized by TEM (H-7650, Hitachi), and the material composition and the crystal structure were acquired by XRD (D8 Discover, Bruker) analysis using an X-ray beam with nickel-filtered Cu-K radiation. VSM (EV7, ADE Technologies) was used to record the magnetic susceptibility of Fe_3O_4 and PVA-Fe_3O_4 and a magnet was added for more intuitive results.

2.5. Immobilization of ω-TA by magnetic PVA-Fe_3O_4 nanoparticles combined with glutaraldehyde

Two gram of magnetic PVA-Fe_3O_4 nanoparticles was added into 17 mL of pH 7.0 phosphate buffer and dispersed by ultrasonic for 20 min. The solution was suspended into the dispersion medium consisted of 200 mL of edible oil, 3 mL of Tween 80 and 30 mL of *n*-butanol under mechanical stirring at 70 °C for 4 h. Glutaraldehyde was then added to a final concentration of 0.05%. Finally, the product was separated and rinsed repeatedly with methanol for getting rid of the remaining dispersion medium. The immobilization of ω-TA onto the magnetic PVA-Fe_3O_4 nanoparticles was carried out by directly adding 1 mL of 1 mg/mL ω-TA (0.3U) to 3 mL of 10 mg/mL magnetic PVA-Fe_3O_4 nanoparticles in 1 mL of pH 7.0 phosphate buffer. After 6 h of reaction, the precipitates were collected using a magnetic field and rinsed 3 times with distilled water and stored at 4 °C until use.

2.6. Determination of activity and concentration of ω-TA

The determination of ω-TA activity was conducted as follows: 1 mL of mixture including 1 mM *R*-α-MBA, 1 mM pyruvate, 0.1 mM PLP, 35 mg of immobilized or 1 mg of free enzymes and phosphate buffer (pH 7.0, 50 mM). After the mixture was incubated at 30 °C and 180 rpm for 10 min, the reaction was stopped by addition of an equal volume of TFA. The mixture was analyzed by HPLC (1500, Alltech)

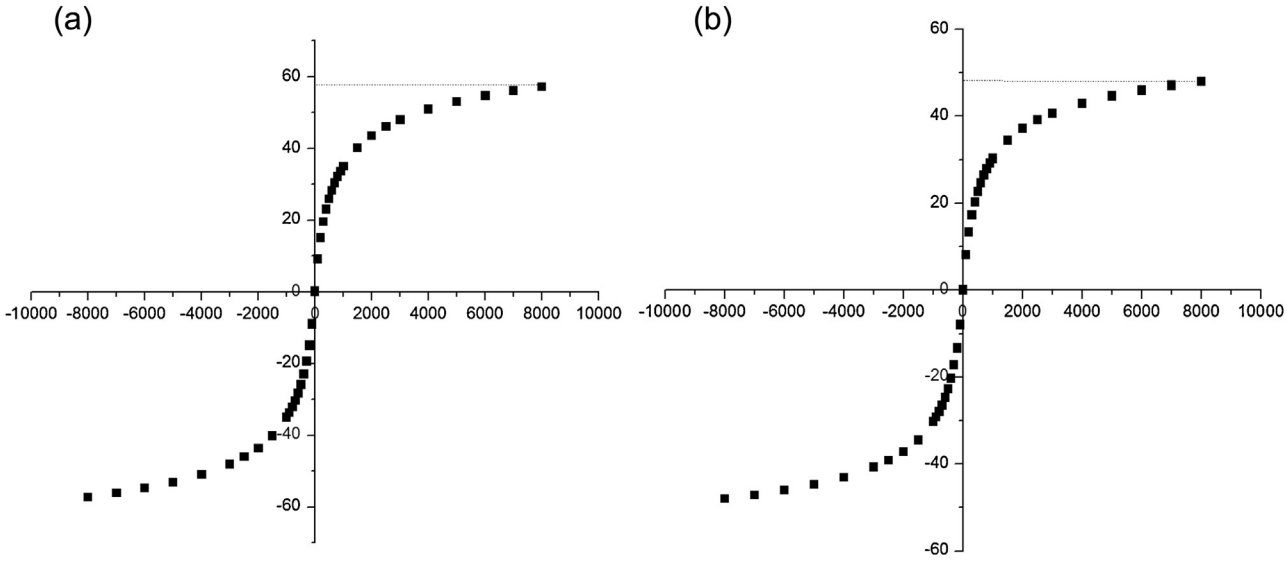

Fig. 1. The hysteresis loop of magnetic nanoparticles: (a) Fe_3O_4; (b) PVA-Fe_3O_4.

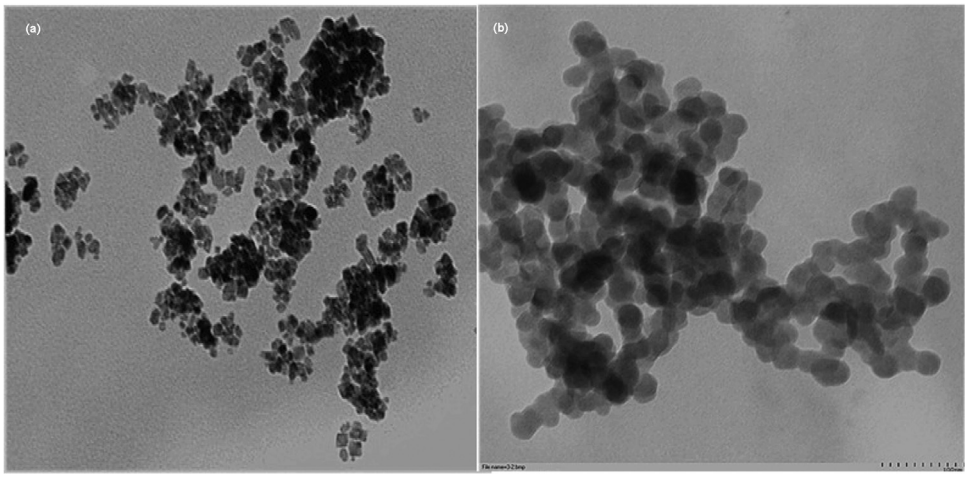

Fig. 2. TEM images of magnetic nanoparticles: (a) Fe_3O_4; (b) PVA-Fe_3O_4.

using a chiral column (CROWNPAK CR(+), 5 μm, 4 × 150 mm, DAICEL) at 220 nm with the elution of 20% purified water and 80% $HClO_4$ buffer (pH 1.5). One unit of ω-TA was defined as the amount of enzyme releasing 1 μmol acetophenone using *R*-α-MBA as substrate per minute at 30 °C.

2.7. Optimum pH, temperature and stability of the free and immobilized ω-TA

Optimum pH of free and immobilized ω-TA was determined at 30 °C in buffer at pH ranging from 4.0 to 9.0 for 12 h, and optimum temperature was determined in phosphate buffer (pH 7.0) at temperature ranging from 20 to 80 °C. Thermal stability of free and immobilized ω-TA was studied at 60 °C in phosphate buffer (pH 7.0) for different time.

2.8. Reusability of the immobilized ω-TA

The reusability of immobilized ω-TA was investigated by converting *R*-α-MBA repeatedly. The reaction solution was consisted of 250 mM *R*-α-MBA, 250 mM pyruvate, 1 mg/mL ω-TA and 0.1 mM PLP. Reaction was conducted at 40 °C for 25 h. After each test, the immobilized ω-TA was collected by using magnetic field and washed three to five times with methanol and distilled water before the next cycle.

3. Results and discussion

3.1. Hysteresis loop analysis

Based on modified co-precipitation and microemulsion method in this paper [24–26], single dispersion, uniform size of the magnetic Fe_3O_4 and PVA-Fe_3O_4 nanoparticles were prepared [27–29]. The hysteresis loop of the magnetic Fe_3O_4 nanoparticles revealed a ferromagnetic behavior and the remanence and coercive force was very small, almost near to zero, closing to super-paramagnetism with the saturated magnetic intensity value of 57.24 emu/g, as can be seen from Fig. 1a. Similarly, the magnetic PVA-Fe_3O_4 nanoparticles also showed that there was no remanence and the coercive force was near to zero. However, the saturated magnetic intensity of the magnetic PVA-Fe_3O_4 nanoparticles had a value as 47.84 emu/g, indicating that the saturated

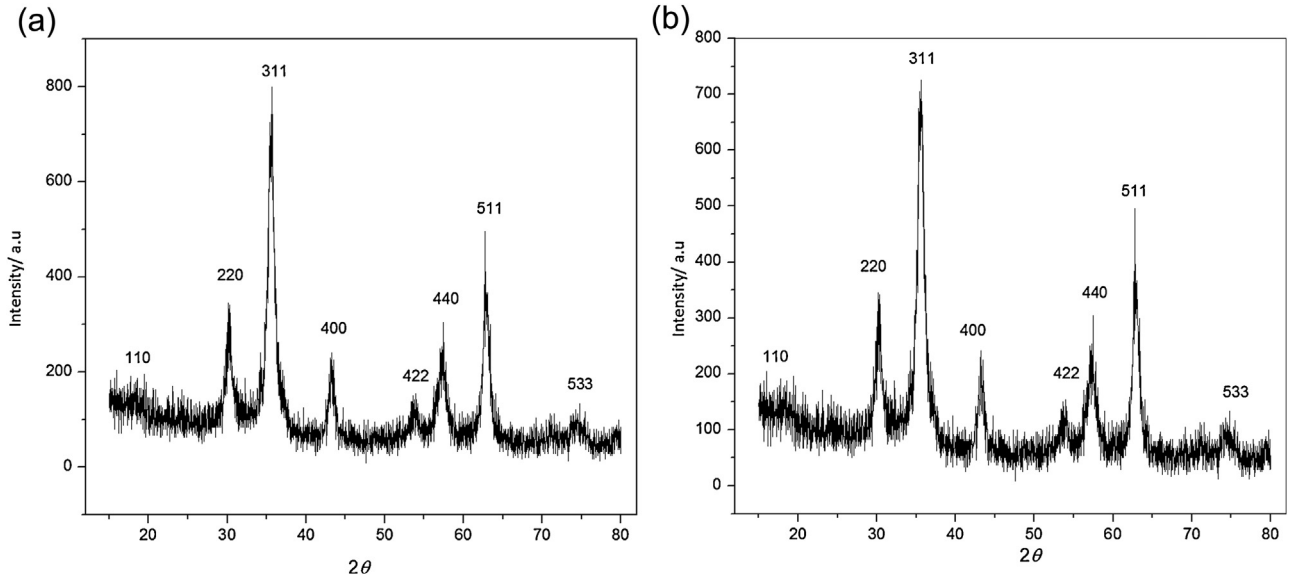

Fig. 3. X-ray diffraction patterns of magnetic nanoparticles (a) Fe_3O_4; (b) PVA-Fe_3O_4.

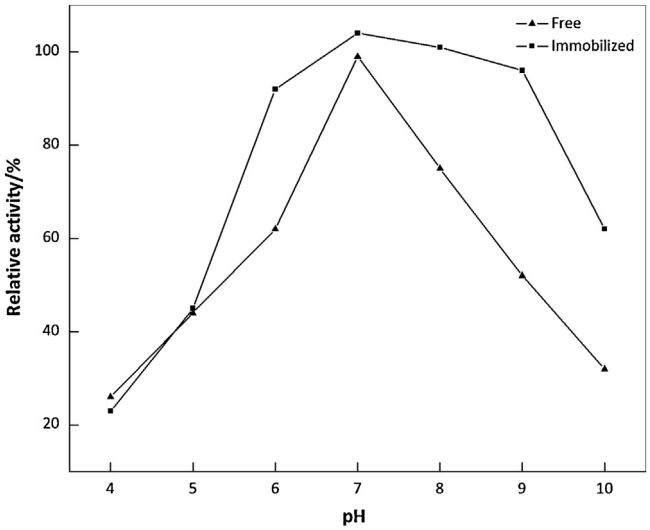

Fig. 4. Optimum pH of the free and immobilized ω-TA.

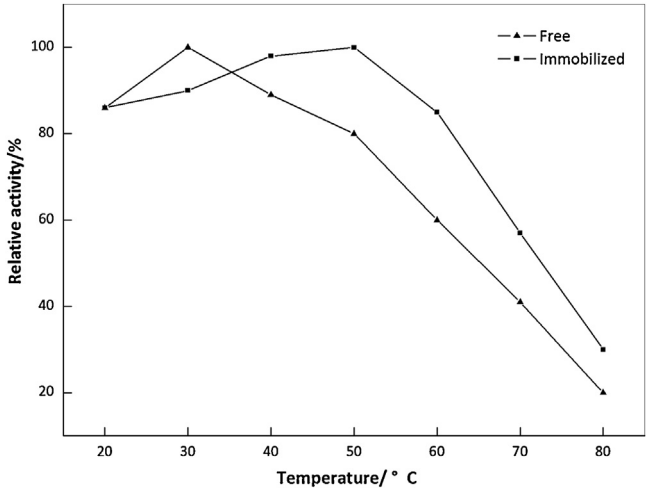

Fig. 5. Optimum temperature of the free and immobilized ω-TA.

magnetic intensity of PVA modified nanoparticles was smaller than that of the unmodified. Similar observations of magnetic chitosan-caoted Fe_3O_4 nanoparticles were presented in previous papers [30,31].

3.2. Magnetic nanoparticles by TEM analysis

In view of the existence of agglomeration, the magnetic nanoparticles would reunit more or less. As is shown in Fig. 2a, the magnetic Fe_3O_4 particles showed its form as not very regular cube, and its diameter was between 10 and 15 nm. Magnetic PVA-Fe_3O_4 nanoparticles were presented in Fig. 2b, and the formation and dispersion of the nanoparticles were clearly observed and particle size distributed in 30–40 nm, which was consistent with the reported coated magnetic naoparticles [30]. Not only had the Fe_3O_4 nanoparticles been stabilized by wrapping PVA in their surface to prevent them from coagulation, but the affinity of the nanoparticles to the cross linker had also been enhanced.

Table 1
Kinetic parameters of the free and immobilized ω-TA.

ω-TA	K_m (mM)	K_{cat} (s^{-1})	K_{cat}/K_m ($mM^{-1}\,s^{-1}$)
Free	4.40 ± 0.13	0.81 ± 0.21	0.18
Immobilized	11.03 ± 0.06	1.52 ± 0.03	0.14

3.3. Magnetic nanoparticles by XRD analysis

To analyze the crystallographic structure of the magnetic nanoparticles, the XRD analysis was performed and results were shown in Fig. 3. The peaks of magnetic Fe_3O_4 nanoparticles respectively corresponded to the standard peaks of Fe_3O_4 characteristic diffraction. The well-defined XRD pattern indicating the formation of magnetic Fe_3O_4 nanoparticles was high purity with a spinel structure [32]. The calculated average particles diameter was 13.53 nm according to the Debye–Scherer's formula. The XRD pattern of magnetic PVA-Fe_3O_4 nanoparticles as is shown in Fig. 3b indicated the characteristic peaks were almost identical to the standard XRD patterns of Fe_3O_4 with 31.45 nm of mean calculated diameter, indicating that it also kept the type of Fe_3O_4. The diameter sizes of both magnetic Fe_3O_4 and PVA-Fe_3O_4 nanoparticles were very close to the results of TEM analysis.

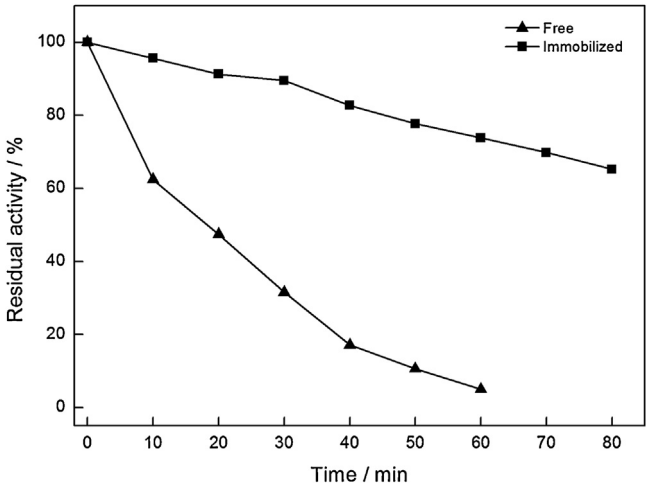

Fig. 6. Thermal stability of the free and immobilized ω-TA.

3.4. Optimum pH and temperature

It is well known that the activity of enzyme depends greatly on the surrounding pH and temperature. Many studies have revealed that the PVA can slightly broaden pH-ranges of the immobilized enzymes [33,34]. As can be seen in Fig. 4, the free ω-TA gave the maximal activity at pH 7.0, but the immobilized ω-TA exhibited much broader optimum pH range within 7.0–9.0. Similar results have been reported for ω-TA immobilized on calcium alginate and chitosan [5–7]. The possible reason was speculated as: PVA could maintain the pH value of microenvironment at a level different from the external medium [35]. The temperature profiles for the free and immobilized ω-TA preparations were shown in Fig. 5. The optimum temperature of the free ω-TA was approximately 30 °C, and it would shift to 40–50 °C for the immobilized one, indicating that the immobilized ω-TA was less sensitive to temperature changes compared to the free one. The enhances optimum temperature have also been currently reported in other studies [5,7,36].

3.5. Kinetic parameters of ω-TA

The K_m and V_{max} are the important kinetic parameters of enzyme and can be calculated from a Lineweaver–Burk plot. The kinetic parameters of the free and immobilized ω-TA were summarized in Table 1. There was an increase in K_m and K_{cat} from the free ω-TA to the immobilized one. The K_m of the free and immobilized ω-TA was 4.40 mM and 11.03 mM, respectively. As a parameter reflecting the affinity between substrate and enzyme, the bigger K_m caused by the increased diffusion and strict resistance of the immobilized ω-TA would lead to the reduced affinity with respect to the free one [35]. Besides, the high hydrophilicity of PVA could also contribute to a higher K_m by reducing the local concentration of substrate in the microenvironment surrounding enzyme [37].

3.6. Thermal stability

Thermal stability of the free and immobilized was tested after incubation in a water bath at 60 °C. In general, the structure of protein would change to various degrees, and then denatures to inactivation with the increased temperature and extension of time. It was clearly shown in Fig. 6 that the activity of the free ω-TA declined to 10% within 60 min, while the immobilized one still retained around 70% residual activity even for 80 min. The effect on thermal stability of immobilized ω-TA was in accordance with results reported in previous article [5]. This might be explained by a covalent bond connection between the enzyme and magnetic PVA-Fe_3O_4 nanoparticles, bringing the immobilized ω-TA a more

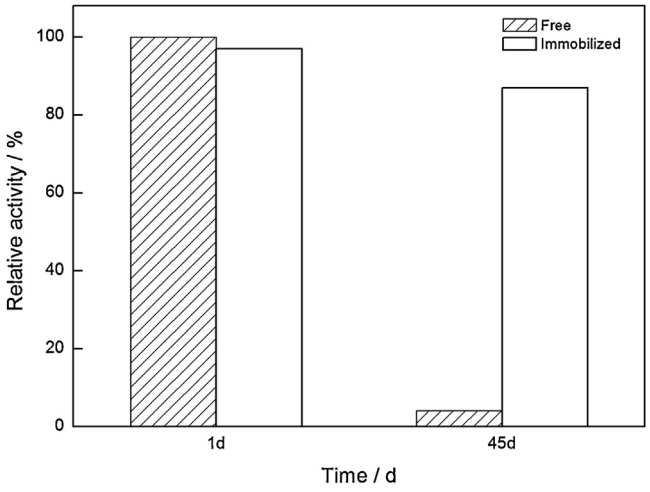

Fig. 7. Storage stability of the free and immobilized ω-TA.

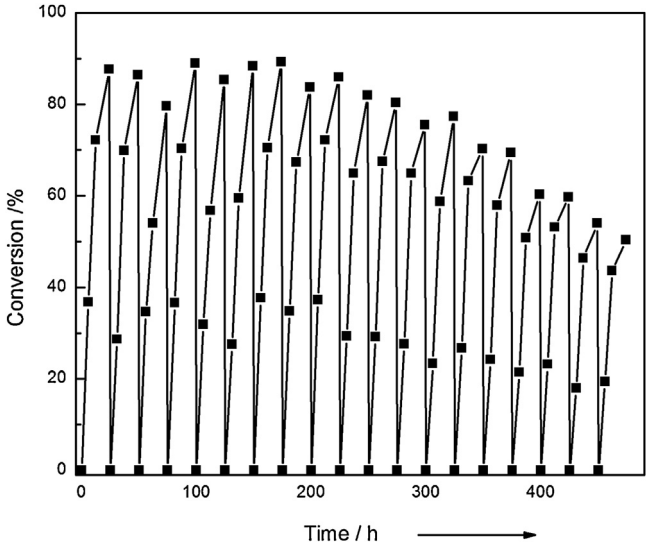

Fig. 8. Reusability experiments of immobilized ω-TA.

inflexibility against the structural changes exposed in heat surroundings [38].

3.7. Storage stability

The residual activities were investigated to examine the storage stability of the free and immobilized ω-TA after stored at 4 °C for 45 days. As shown in Fig. 7, the free ω-TA presented no detectable activity, and the immobilized one was found to maintain more than 80% residual activity. This result was identical to previous reports about immobilization of ω-TA and other enzymes [8,20,36].

3.8. Reusability

Reusability is an important criterion of enzyme for industrial utilization. The immobilized ω-TA was performed to convert *R*-α-MBA for 19 consecutive reaction cycles over 475 h under the same conditions. Results showed the immobilized ω-TA might present almost no decrease in activity after 13 rounds of operation. Conversion rate of nearly 50% could be remained after 19 rounds. Compared to the immobilized ω-TA reported in previous publications [8–10,39], a better operational stability would be apparently achieved in this paper (Fig. 8).

4. Conclusion

In this paper, the magnetic PVA-Fe_3O_4 nanoparticles with average size between 30 and 40 nm were synthesized and used as carrier for immobilization of ω-TA. The immobilized ω-TA, with broader pH range and higher optimum temperature, might present better thermal and storage stability. It could be successfully reused for 13 cycles with high activity being retained. The immobilized ω-TA could be a promising biocatalyst for kinetic resolution of chiral amines.

Acknowledgements

The research was financially supported by NSFC (20906048), the State Key Basic Research and Development Plan of China (2009CB724700) and a project funded by the Priority Academic Program Development of Jiangsu Higher Education Institutions (PAPD).

References

[1] D. Koszelewski, K. Tauber, K. Faber, W. Kroutil, ω-Transaminases for the synthesis of non-racemic α-chiral primary amines, Trends Biotechnol. 28 (2010) 324–332.
[2] B.K. Cho, H.Y. Park, J.H. Seo, J. Kim, T.J. Kang, B.S. Lee, B.G. Kim, Redesigning the substrate specificity of ω-aminotransferase for the kinetic resolution of aliphatic chiral amines, Biotechnol. Bioeng. 99 (2008) 275–284.
[3] S. Mathew, H. Yun, ω-Transaminases for the production of optically pure amines and unnatural amino acids, ACS Catal. 2 (2012) 993–1001.
[4] B.Y. Hwang, H.Y. Park, B.S. Lee, Identification of ω-Aminotransferase from Caulobacter crescentus and site directed mutagenesis to broaden substrate specificity, J. Mol. Microbiol. Biotechnol. 18 (2008) 48–54.
[5] C.K. Savile, J.M. Janey, E.C. Mundorff, J.C. Moore, S. Tam, W.R. Jarvis, J.C. Colbeck, A. Krebber, F.J. Fleitz, J. Brands, P.N. Devine, Biocatalytic asymmetric synthesis of chiral amines from ketones applied to sitagliptin manufacture, Science 329 (2010) 305–309.
[6] T. Pär, L. Joana, S. Jacob, A. Naweed, N. Watson, M. John, Process considerations for the asymetric synthesis of chiral amines using transaminases, Biotechnol. Bioeng. 108 (2011) 1479–1493.
[7] A.R. Martin, D. Shonnard, S. Pannuri, S. Kamat, Characterization of free and immobilized (*S*)-aminotransferase for acetophenone production, Appl. Microbiol. Biotechnol. 76 (2007) 843–851.
[8] S. Yi, C. Lee, J. Kim, D. Kyung, B. Kim, Y. Lee, Covalent immobilization of ω-transaminase from Vibrio fluvialis JS17 on chitosan beads, Process Biochem. 42 (2007) 895–898.
[9] H. Mallin, U. Menyes, T.T. Vorhaben, M.H.O. Hne, U.T. Bornscheuer, Immobilization of two (*R*)-amine transaminases on an optimized chitosan support for the enzymatic synthesis of optically pure amines, ChemCatChem 5 (2013) 588–593.
[10] M. Päiviö, L.T. Kanerva, Reusable ω-transaminase sol–gel catalyst for the preparation of amine enantiomers, Process Biochem. 48 (2013) 1488–1494.
[11] M.D. Truppo, H. Strotman, G. Hughes, Development of an immobilized transaminase capable of operating in organic solvent, ChemCatChem 4 (2012) 1071–1074.
[12] M. Cardenas-Fernandez, W. Neto, C. Lopez, G. Alvaro, P. Tufvesson, J.M. Woodley, Immobilization of *Escherichia coli* containing omega-transaminase activity in LentiKats®, Biotechnol. Prog. 28 (2012) 693–698.
[13] G. Rehn, C. Grey, C. Branneby, L. Lindberg, P. Adlercreutz, Activity and stability of different immobilized preparations of recombinant *E. coli* cells containing omega-transaminase, Process Biochem. 47 (2012) 1129–1134.
[14] S.A. Ansari, Q. Husain, Potential applications of enzymes immobilized on/in nano materials: a review, Biotechnol. Adv. 30 (2012) 512–523.
[15] P. Wang, Nanoscale engineering for smart biocatalysts with fine-tuned properties and functionalities, Top. Catal. 55 (2012) 1107–1113.
[16] Y. Zhu, S. Kaskel, J. Shi, T. Wage, K.H. van Pée, Immobilization of *Trametes versicolor* laccase on magnetically separable mesoporous silica spheres, Chem. Mater. 19 (2007) 6408–6413.
[17] A.C. Patel, S. Li, J. Yuan, Y. Wei, In situ encapsulation of horseradish peroxidase in electrospun porous silica fibers for potential biosensor applications, Nano Lett. 6 (2006) 1042–1046.
[18] Y. Song, F. Schmidt-Stein, S. Berger, P. Schmuki, TiO_2 nano test tubes as a self-cleaning platform for high-sensitivity immunoassays, Small 6 (2010) 1180–1184.

[19] H.H.P. Yiu, M.A. Keane, Enzyme-magnetic nanoparticle hybrids: new effective catalysts for the production of high value chemicals, J. Chem. Technol. Biotechnol. 87 (2012) 583–594.
[20] F. Wang, C. Guo, H.Z. Liu, C.Z. Liu, Immobilization of *Pycnoporus sanguineus* laccase by metal affinity adsorption on magnetic chelator particles, J. Chem. Technol. Biotechnol. 83 (2008) 97–104.
[21] F. Sulek, M. Drofenik, M. Habulin, Z. Knez, Surface functionalization of silica-coated magnetic nanoparticles for covalent attachment of cholesterol oxidase, J. Magn. Magn. Mater. 322 (2010) 179–185.
[22] G.Y. Li, Z.D. Zhou, Y.J. Li, K.L. Huang, M. Zhong, Surface functionalization of chitosan-coated magnetic nanoparticles for covalent immobilization of yeast alcohol dehydrogenase from *Saccharomyces cerevisiae*, J. Magn. Magn. Mater. 322 (2010) 3862–3868.
[23] W. Xie, N. Ma, Enzymatic transesterification of soybean oil by using immobilized lipase on magnetic nano-particles, Biomass Bioenergy 34 (2010) 890–896.
[24] C. Pan, B. Hu, W. Li, Y. Sun, H. Ye, X. Zeng, Novel and efficient method for immobilization and stabilization of β-d-galactosidase by covalent attachment onto magnetic Fe_3O_4–chitosan nanoparticles, J. Mol. Catal. B 61 (2009) 208–215.
[25] H. Xu, L. Cui, N. Tong, H. Gu, Development of high magnetization Fe_3O_4/polystyrene/silica nanospheres via combined miniemulsion/emulsion polymerization, J. Am. Chem. Soc. 128 (2006) 15582–15583.
[26] D. Zhang, A.B. Karki, D. Rutman, D.P. Young, A. Wang, D. Cocke, T.H. Ho, Z.H. Guo, Electrospun polyacrylonitrile nanocomposite fibers reinforced with Fe_3O_4 nanoparticles: fabrication and property analysis, Polymer 50 (2009) 4189–4198.
[27] W. Ding, S.Y. Wei, J.H. Zhu, X.L. Chen, D. Rutman, Z.H. Guo, Manipulated electrospun PVA nanofibers with inexpensive salts, Macromol. Mater. Eng. 295 (2010) 958–965.
[28] Z. Wang, A.B. Karki, Y.H. Li, P. Bernazzani, D.P. Young, J.A. Gomes, D.L. Cocke, T.C. Ho, Z.H. Guo, D. Zhang, S.Y. Wei, Effects of iron oxide nanoparticles on polyvinyl alcohol: interfacial layer and bulk nanocomposites thin Film, J. Nanopart. Res. 12 (2010) 2415–2426.
[29] E. Atabey, S.Y. Wei, X. Zhang, H.B. Gu, X.R. Yan, Y.D. Huang, L. Shao, Q.L. He, J.H. Zhu, L.Y. Sun, A.S. Kucknoor, A. Wang, Z.H. Guo, Fluorescent electrospun polyvinyl alcohol CdSe ZnS nanocomposite fibers, J. Compos. Mater. 47 (2013) 3175–3185.
[30] V. Kumar, F. Jahan, S. Raghuwanshi, R.V. Mahajan, R.K. Saxena, Immobilization of *Rhizopus oryzae* lipase on magnetic Fe_3O_4-chitosan beads and its potential in phenolic acids ester synthesis, Biotechnol. Bioprocess Eng. 18 (2013) 787–795.
[31] C.H. Kuo, Y.C. Liu, C.M.J. Chang, J.H. Chen, C. Chang, C.J. Shieh, Optimum conditions for lipase immobilization on chitosan-coated Fe_3O_4 nanoparticles, Carbohydr. Polym. 87 (2012) 2538–2545.
[32] Z.Y. Ma, Y.P. Guan, H.Z. Liu, Synthesis and characterization of micron-sized monodisperse superparamagnetic polymer particles with amino groups, J. Polym. Sci. A 43 (2005) 3433–3439.
[33] A. Dinçer, A. Telefoncu, Improving the stability of cellulase by immobilization on modified polyvinyl alcohol coated chitosan beads, J. Mol. Catal. B 45 (2007) 10–14.
[34] K.S. Atia, S.A. Ismail, A.M. Dessouki, Immobilization of β-amylase using polyacrylamide polymer derivatives, J. Chem. Technol. Biotechnol. 78 (2003) 891–898.
[35] K.S. Atia, A.I. El-Batal, Preparation of glucose oxidase immobilized in different carriers using radiation polymerization, J. Chem. Technol. Biotechnol. 80 (2005) 805–811.
[36] F. Kartal, A. Akkaya, A. Kilinc, Immobilization of porcine pancreatic lipase on glycidyl methacrylate grafted poly vinyl alcohol, J. Mol. Catal. B 57 (2009) 55–61.
[37] A.M. Dessouki, K.S. Atia, Immobilization of adenosine deaminase onto agarose and casein, Biomacromolecules 3 (2002) 432–437.
[38] E. Taqieddin, M. Amiji, Enzyme immobilization in novel alginate–chitosan core–shell microcapsules, Biomaterials 25 (2004) 1937–1945.
[39] K. Ni, Z. Zhou, L. Zhao, H. Wang, Y. Ren, D. Wei, Magnetic catechol-chitosan with bioinspired adhesive surface: preparation and immobilization of ω-transaminase, PLoS One 7 (2012) e41101.